Acc. Chem. Res. **2001,** *34,* 159−170

Dynamics of Photoinduced Charge Transfer and Hole Transport in Synthetic DNA Hairpins

FREDERICK D. LEWIS,*
ROBERT L. LETSINGER, AND
MICHAEL R. WASIELEWSKI
Department of Chemistry, Northwestern University, Evanston, Illinois 60208

Received August 1, 2000

ABSTRACT
The dynamics of photoinduced charge separation and charge recombination processes in synthetic DNA hairpins have been investigated by means of femtosecond transient absorption spectroscopy. The driving force and distance dependence of charge-transfer processes involving singlet acceptors and nucleobase donors are consistent with a single-step superexchange mechanism in which the electronic coupling between the donor and acceptor is strongly distance dependent. The dynamics of reversible hole transport between a primary guanine donor and nearby GG or GGG sequences has also been determined and establishes that these sequences are very shallow hole traps.

Introduction

The hydrogen-bonded base pairs which constitute the core of duplex DNA form an extended one-dimensional π-stacked array with an average stacking distance of 3.4 Å.[1] This ordered structure is found nowhere else in nature and thus has a special fascination for both biologists and chemists. The possibility that the π-stacked base pairs of DNA might serve as a pathway for charge transport was advanced over 30 years ago.[2] Interest in the electronic properties of DNA has been stimulated by Barton and Turro's proposal that DNA serves as a molecular wire or "π-way".[3−5] The advent of molecular electronics has further fueled interest in the potential role of DNA as a molecular wire.[6−8] There is no evidence that charge-transport processes are involved in the storage of genetic information by DNA. However, such processes have been implicated in a variety of oxidative processes which ultimately lead to mutations, compromising the biological function of DNA.[9,10] Thus, elucidation of the mechanism and dynamics of these processes is of fundamental importance to understanding DNA oxidative damage and to the design of DNA-based molecular devices.

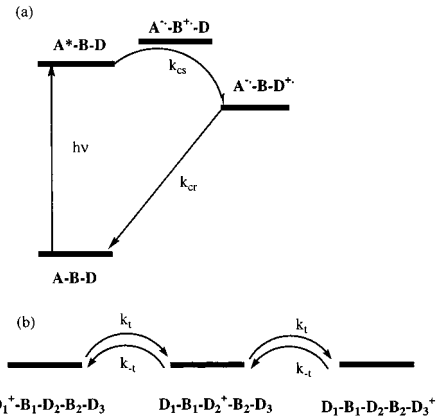

FIGURE 1. Energy level diagram for (a) photoinduced charge separation and charge recombination in an acceptor−bridge−donor (A−B−D) system and (b) hole transport between donors D_1, D_2, and D_3 separated by bridges B_1 and B_2.

During the past decade, photochemical methods have been widely used to study charge-transfer processes in DNA.[11−17] Photoinduced charge transfer offers several advantages over the use of chemical oxidants or ionizing radiation, including site-specificity and dynamic measurements with femtosecond time resolution. Experimental investigations and theoretical treatments of photoinduced charge transfer in DNA have revealed the occurrence of at least two mechanisms, a single-step superexchange mechanism which is strongly distance dependent, and a multistep hole-hopping mechanism which is only weakly distance dependent.[18−25] These mechanisms are shown schematically in Figure 1. In the superexchange mechanism (Figure 1a) one or more π-stacked base pair serves as a bridge (B) separating the electron acceptor (A) and donor (D). The rate constant for charge separation (k_{cs}) can be described in simplest form by eq 1, where R is the

$$k_{cs} = k_o\, e^{-\beta R} \qquad (1)$$

D−A center-to-center distance and β is dependent upon the nature of the bridge and its coupling with D and A.[19] In the hopping mechanism (Figure 1b), a hole generated either chemically or photochemically can reversibly hop from one donor site to another until it reaches a trap site. If each hopping step is treated as a superexchange process,

Frederick D. Lewis was born in Boston, MA. He received his B.A. degree from Amherst College in 1965 and his Ph.D. from the University of Rochester in 1968. Following a postdoctoral appointment at Columbia University with N. J. Turro, he joined the faculty of Northwestern University in 1969. He is currently serving as President of the Inter-American Photochemical Society. His research interests are focused on the relation between photochemical behavior and molecular structure in systems ranging from small molecules to DNA.

Robert L. Letsinger was born in Bloomfield, IN. He received his B.S. degree in 1943 and his Ph.D. in 1945, both from MIT. He joined the faculty of Northwestern University in 1946 and is currently Clare Hamilton Hall Professor, Emeritus. He is best known for his pioneering studies in solid-phase synthesis and nucleic acid chemistry. His achievements have been recognized by election to the Nation Academy of Sciences and numerous awards, including the American Chemical Society A. C. Cope Scholar Award. His current interests include nanotechnology and its applications to DNA diagnostics.

Michael R. Wasielewski was born in Chicago, IL. He received his B.S. degree in 1971 and his Ph.D. in 1975, both from the University of Chicago. Following postdoctoral studies with R. Breslow at Columbia, he joined the scientific staff of the Chemistry Division of the Argonne National Laboratory. In 1994 he joined the faculty of Northwestern University, where he is Professor of Chemistry. He held a joint appointment at Argonne until 1999, when all of his research activities moved to Northwestern. His research focuses on electron-transfer reactions, the synthesis of donor−acceptor molecules and materials, ultrafast photophysical and photochemical processes in organic molecules and optoelectronic materials, magnetic properties of radical ion pairs, and the primary events of photosynthesis.

10.1021/ar0000197 CCC: $20.00
Published on Web 12/13/2000

then the rate constant can be described by eq 2, where N

$$k_{hop} = PN^{-\eta} \quad (2)$$

is the number of hopping steps and η has a value between 1 and 2.[24,25] In addition, a single-step mechanism that is not strongly dependent upon distance has been proposed by Barton and Turro[5] and an elaborated hopping mechanism described as "phonon-assisted polaron-like hopping" advanced by Schuster.[16] These proposals have generated a lively controversy and have attracted the attention of the popular science press.[26−28]

Our interest in photoinduced charge transfer in DNA was stimulated by investigations of the synthesis and properties of hairpin-forming bis(oligonucleotide) conjugates in one of our laboratories.[29,30] Hairpins in which a stilbene-4,4′-dicarboxamide (SA) serves as a linker connecting complementary polyT and polyA arms are strongly fluorescent, whereas hairpins with polyC−polyG arms are totally nonfluorescent.[30] Quenching of SA fluorescence by G:C but not A:T base pairs appeared to be consistent with an electron-transfer mechanism in which the SA linker served as an electron acceptor and guanine, the most easily oxidized nucleobase, as the electron donor.

At the time we initiated our collaborative investigation of photoinduced charge transfer in DNA in 1996, there were no direct measurements of the distance or driving force dependence of the dynamics of electron-transfer processes in structurally well-defined models for duplex DNA. Studies of photoinduced electron transfer using randomly intercalated donors and acceptors[3,4,31] yielded conflicting results, as did studies using tethered donors and acceptors separated by a single fixed base sequence.[32,33] The SA-linked hairpins provided a system that enabled us to investigate the distance dependence of single-step charge separation and charge recombination processes in which the singlet linker serves as the acceptor and a single guanine as the donor. This study provided the first experimental value of the distance dependence of electron transfer in DNA, $\beta = 0.64$ Å^{-1},[34,35] a value toward which subsequent results from other laboratories for related systems appear to be converging. Variation in the linker acceptor and nucleobase donor enabled us to determine the driving force dependence of the dynamics of electron transfer in DNA,[36] thereby providing intimate details about DNA as a medium for electron transfer. In addition, investigations of the dynamics of charge recombination in more complex systems containing multiple guanine donors permitted us to obtain the first measurements of the dynamics and equilibria for hole transport in DNA.[37,38]

Synthesis, Structure, and Properties of DNA Hairpins

The stilbenedicarboxamide (SA) synthon used in the preparation of SA-linked hairpins is obtained from stilbene-4,4′-dicarboxylic acid via reaction of its acid chloride with 3-hydroxy-1-propylamine.[30] This method is readily adapted to the synthesis of linkers derived from the

Chart 1. Structures, Singlet Energies, and Redox Potentials of Linker Diols

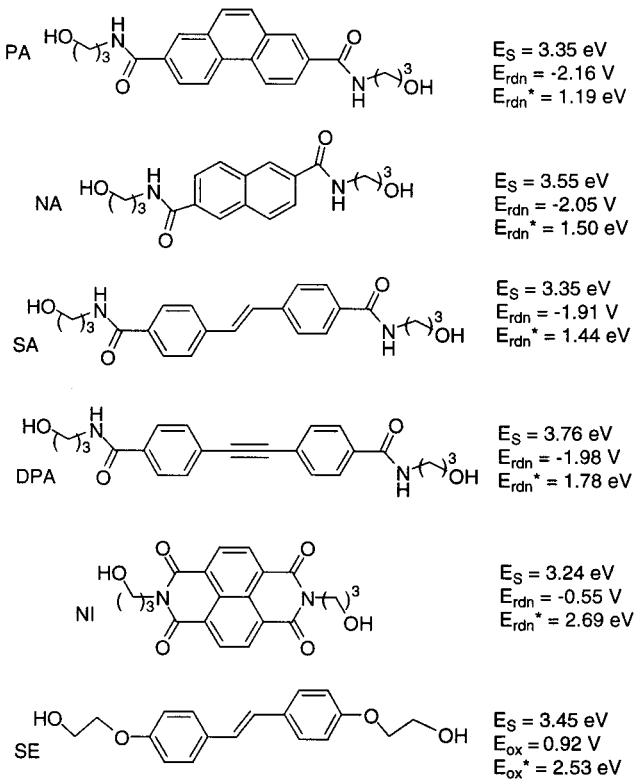

dicarboxylic acids of phenanthrene (PA),[36] naphthalene (NA),[39] and diphenylacetylene (DPA).[40] We have also prepared linkers containing a naphthalenediimide (NI),[36,41] stilbenediether (SE),[42,43] and ruthenium tris(bipyridyl) chromophores.[44] The linker diol derivatives whose structures are shown in Chart 1 are all strongly fluorescent. Their singlet energies and ground-state reduction or oxidation potentials are reported in Chart 1 along with their excited-state redox potentials ($E_{rdn}^* = E_S + E_{rdn}$ or $E_{ox}^* = E_S - E_{ox}$).[45] Bis(oligonucleotide) conjugates are prepared via conventional phosphoramidite chemistry using the monoprotected (as the (4,4′-dimethoxytriphenylmethyl)ether derivative), monoactivated (as the phosphoramidite) diol synthon.[30] By varying the order of introduction of nucleotides, it is possible to prepare several hairpins containing the same linker in a single day. In addition to the four common nucleobases, we have employed several nucleobase analogues including 2-bromouracil, inosine, deazaguanine, and 8-oxoguanine. Their structures, letter codes, and oxidation and reduction potentials are provided in Chart 2.[45,46]

The thermal stability of SA-linked hairpins possessing polyT and polyA arms (T_n-SA-A_n) increases with the number of A:T base pairs (T_M = melting temperature, Chart 3).[30] Substitution of a G:C base pair for a T:A base pair results in an increase in melting temperature. Hairpin thermal stability is also dependent upon linker design. The most stable hairpins that we have studied to date possess a stilbenediether (SE) linker (Chart 3).[42] The melting temperatures of the T_4-SE-A_4 hairpin decrease slightly when the flexible portion of the SE linker is changed from

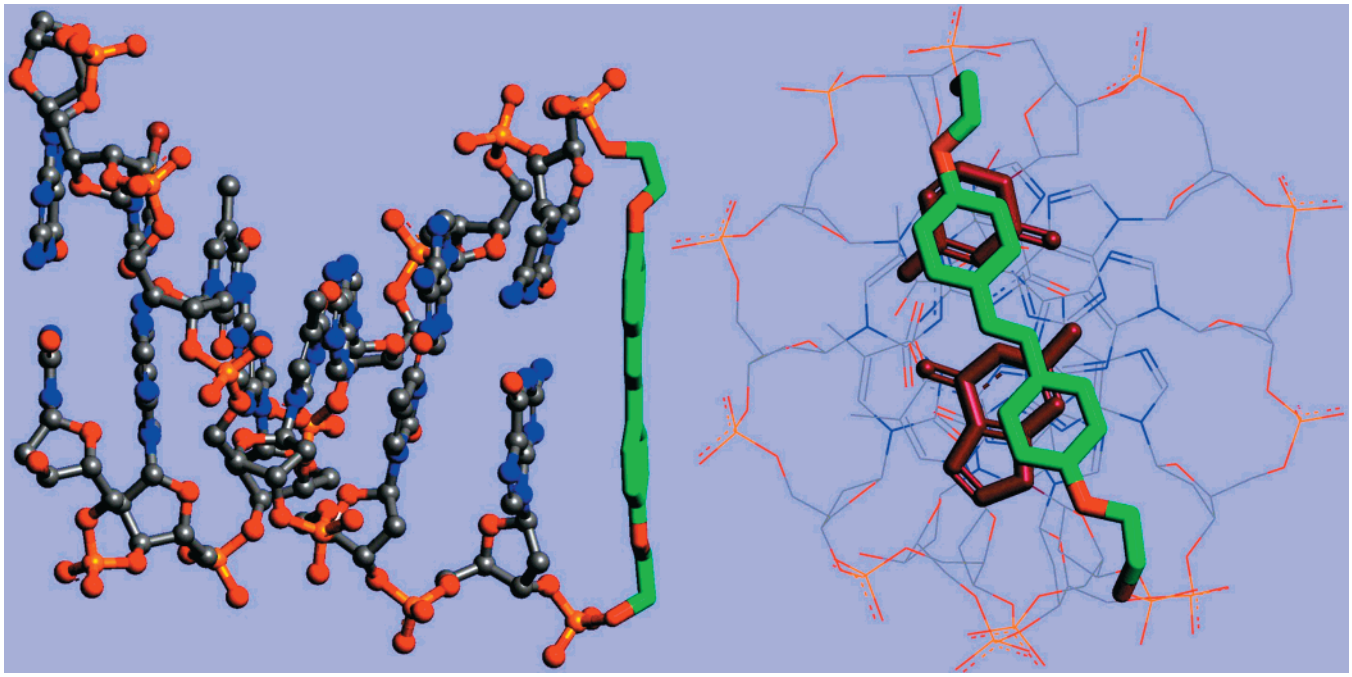

FIGURE 2. Crystal structure of a stilbenediether-linked hairpin. Left: view of the hairpin from the side with stilbene in green on the right. Right: view of the hairpin from the stilbene end with stilbene in green and the nearest-neighbor base pair in red.

Chart 2. Structures and Oxidation and Redox Potentials of Nucleobases

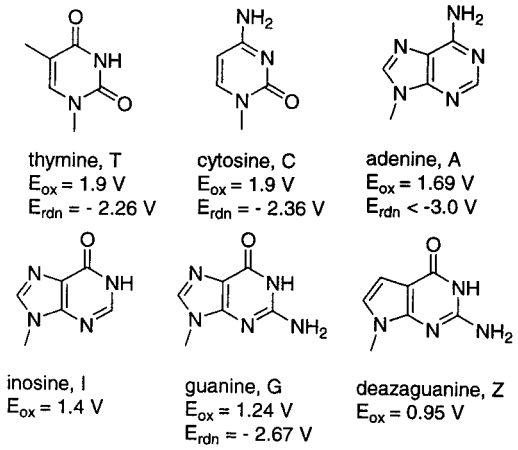

Chart 3. Structures and Melting Temperatures of Hairpins with SA and SE Linkers

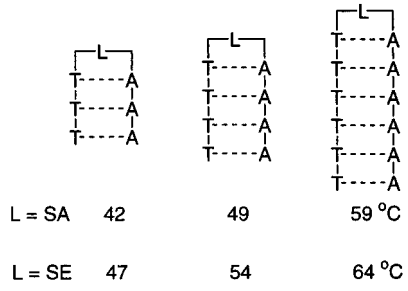

dimethylene to tri- or tetramethylene (T_M = 54, 53, and 48 °C, respectively). A much lower melting temperature is observed for a T_4-SE-A_4 hairpin possessing a *cis*-stilbenediether linker (T_M = 30 °C). This difference in thermal stability has permitted the design of a conjugate which undergoes phototriggered hairpin formation.[43]

The structure of an SE-linked hairpin has been determined by Egli and co-workers.[42] The asymmetric unit consists of four hairpins, each of which adopts a B-form DNA conformation in which the stilbene is π-stacked with the adjacent G:C base pair. The structure of one of the four hairpins in the asymmetric unit is shown in Figure 2. The four hairpins have different sugar−phosphate backbone geometries but similar π-stacking. The dimethylene groups in the SE linkers adopt gauche conformations resulting in an average distance of 18.1 Å for the phosphorus atoms bound to the linker, which is only slightly longer than the average values for the base pairs in the hairpin (17.7 Å). Molecular modeling indicates that hairpins with the other linkers in Chart 1 can also adopt low-energy B-form conformations with calculated chromophore−base pair π-stacking distances between 3.5 and 4.2 Å. The calculated P−P distance for the T_4-SE-A_4 hairpin possessing a *cis*-stilbenediether linker is only 15.4 Å, too short for a stable hairpin geometry.

The absorption and fluorescence spectra of the SA diol linker and the SA-linked hairpin are shown in Figure 3. The SA diol has an allowed π,π^* transition with a maximum at 322 nm in methanol solution. This band is slightly red shifted in the spectrum of the hairpin in aqueous solution. The 260 nm band results from overlapping absorption of the nucleobases and the SA linker. Melting of the hairpin results in ca. 30% hyperchromism at 260 nm but little change in the 330 nm absorbance. The other linkers in Chart 1 also have absorption bands at wavelengths longer than 300 nm, and their hairpins display hypochromism in their 260 nm bands but not in their long-wavelength bands. The CD spectra of the hairpins display a positive band at 283 nm and a negative band at 250 nm typical of B-form DNA, but no CD signals above 300 nm.

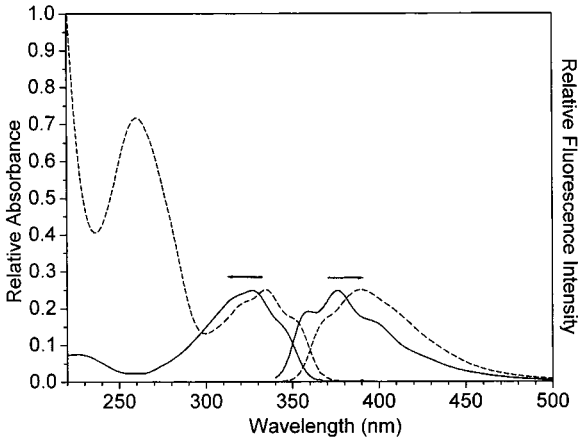

FIGURE 3. Absorption and fluorescence spectra of the stilbene diol linker SA (—) in methanol solution (7.7×10^{-6} M) and an SA-linked hairpin (- - -) in aqueous solution (4.9×10^{-6} M, 0.1 M NaCl, 10 mM sodium phosphate, pH 7.2).

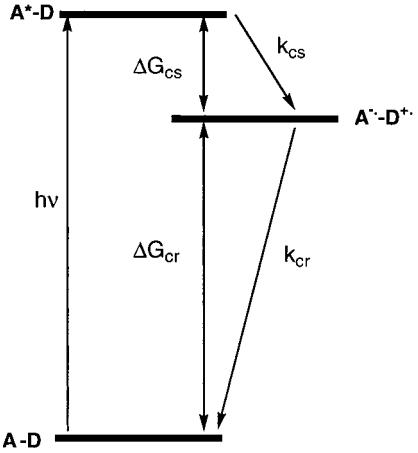

FIGURE 4. Kinetic scheme and thermodynamics of charge separation and charge recombination. A is the acceptor linker chromophore and D is the nucleobase donor.

The SA fluorescence is also slightly red-shifted for the hairpin in aqueous solution vs the diol in methanol (Figure 3).[35] The fluorescence quantum yield of the hairpin T_6-SA-A_6 is substantially larger than that of the SA linker diol ($\Phi_f = 0.38$ vs 0.11), presumably due to the hairpin geometry which inhibits torsion about the stilbene double bond. The increase in Φ_f is accompanied by an increase in SA singlet lifetime, τ_s, from 0.28 ns for the SA linker diol to 2.0 ns for T_6-SA-A_6. A small increase in τ_s is also observed for the hairpin T_6-PA-A_6 vs the PA linker diol ($\tau_s = 25$ vs 18 ns).[36] The fluorescence of the linker chromophore is quenched to a greater or lesser extent in all of the other hairpins studied (vide infra). In all cases for which hairpin fluorescence decays have decay times long enough for us to measure conveniently (>0.1 ns), their decays are found to be single exponential. This indicates that the hairpins adopt a single conformation (or multiple conformations with similar decay times) and greatly simplifies the analysis of fluorescence or transient absorption data.

The modest shifts in the absorption and fluorescence maxima of the linker chromophores upon incorporation into DNA hairpins and the absence of hypochromism or induced circular dichroism indicate that the electronic structure of the chromophore is not strongly perturbed by the neighboring base pair. Evidently, the geometric constraints of the covalent linker assembly and hydrophobic association are sufficient to achieve a loosely π-stacked geometry without significant ground-state electronic interactions such as those present in Mulliken-type ground-state charge-transfer complexes.[47−49]

Electron-Transfer Quenching by Nearest-Neighbor Nucleobases

Whereas the hairpin T_6-SA-A_6 is strongly fluorescent, an analogue which possesses a single G:C base pair adjacent to the chromophore is totally nonfluorescent.[34,35] Quenching of singlet SA by G:C but not A:T base pairs is consistent with an electron-transfer mechanism for fluorescence quenching in which SA serves as an electron acceptor (A*) and guanine as an electron donor (D). Charge separation results in the formation of the radical ion pair $A^{-\bullet}D^{+\bullet}$, which returns to the ground state via charge recombination, as shown schematically in Figure 4.

The energetics of photoinduced charge separation and charge recombination processes can be estimated by using Weller's equations (eqs 3 and 4), where E_{ox} is the

$$\Delta G_{cs} = E_{ox} - E_{red} - E_S + C \quad (3)$$

$$\Delta G_{cr} = E_{red} - E_{ox} \quad (4)$$

nucleobase oxidation potential, E_{red} is the linker reduction potential, E_S is the linker singlet energy, and C is the solvent-dependent Coulombic attraction energy.[50] Values of E_{ox} for the π-stacked bases in the core of DNA have not been measured but are assumed to be similar to those of the individual nucleotides in a polar aprotic solvent such as acetonitrile.[39,46] The value of C in a moderately polar environment is sufficiently small that it can be neglected. The values of ΔG_{cs} calculated for reaction of the SA linker with G and A using the data in Charts 1 and 2 are −0.20 and +0.25 V, respectively, in accord with the observation of efficient fluorescence quenching by G but not by A. Quenching by G but not by A is also observed for hairpins which possess the PA linker, which is a weaker acceptor than is SA.[36] The fluorescence of NA, DPA, and NI linkers, which are stronger acceptors than SA (Chart 1), is quenched by neighboring A:T base pairs as well as G:C base pairs.

Experimental evidence that fluorescence quenching occurs via an electron-transfer mechanism (Figure 4) is provided by subpicosecond time-resolved transient absorption spectroscopy.[34−36,40,42] The spectra obtained for the hairpin T_5-DPA-A_5 are shown in Figure 5.[40] The spectrum obtained 2 ps after the 327 nm excitation pulse is similar in appearance to that of the DPA diol linker and is assigned to the DPA singlet state. This spectrum decays rapidly and is replaced by a new band at shorter wavelength which is assigned to the linker anion radical, $DPA^{-\bullet}$. Decay of both the 535 and 500 nm bands is dominated by a single component, which is assigned to the charge

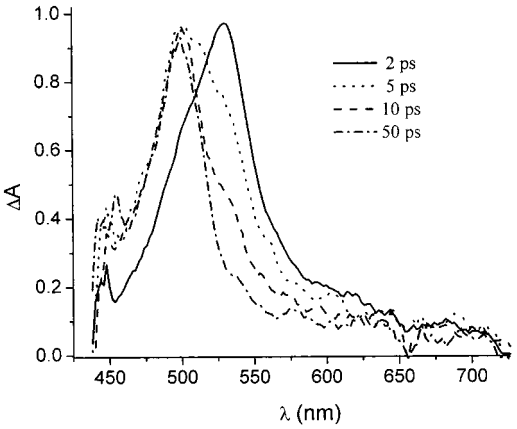

FIGURE 5. Transient absorption spectra of the T_5-DPA-A_5 hairpin obtained after a 0.2 ps, 327 nm excitation pulse at indicated delay times. Spectral intensities are normalized at their maxima.

Chart 4. Structures of Hairpins with Nearest-Neighbor Quenchers

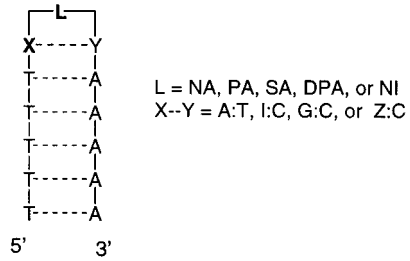

separation and charge recombination processes, respectively. Comparison of the singlet decay time in the absence and in the presence of quencher (τ_s° and τ_s, respectively) provides the rate constant for charge separation ($k_{cs}^{-1} = \tau_s - \tau_s^\circ$), and the rate constant for charge recombination is obtained directly from the anion radical decay time ($k_{cr}^{-1} = \tau_a$). The formation and decay of the linker anion radical have also been observed for SA and NI linkers.[34–36] In all cases the transient absorption spectrum is dominated by the linker anion. The nucleobase cation radicals are known to have broad absorption spectra with much lower absorbance than the SA, DPA, and NI anion radicals.[51]

Driving Force Dependence of Nearest-Neighbor Charge-Transfer Dynamics

Values of k_{cs} and k_{cr} have been determined by means of transient absorption spectroscopy for eight hairpins containing SA, DPI, and NI linkers and various nucleobase donors (Chart 4).[36] In addition, values of k_{cs} have been estimated for hairpins possessing PA and NA linkers from fluorescence decay data. The results are shown in Figure 6. Values of k_{cs} increase rapidly from $\leq 10^7$ s^{-1} for $\Delta G_{cs} = +0.5$ eV to 5×10^{12} s^{-1} for $\Delta G_{cs} = -0.6$ eV but remain fairly constant or decrease slightly for larger driving forces. Values of k_{cr} decrease with increasing driving force, as expected for electron-transfer processes in the Marcus inverted region.[52] The data in Figure 6 can be analyzed within the framework of semiclassical electron-transfer theory using the Marcus-Levich-Jortner equation (eq 5), where $\hbar = h/2\pi$ (h is Planck's constant), k_B is the

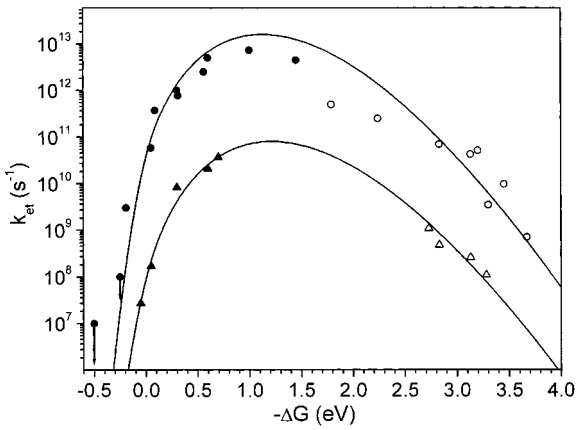

FIGURE 6. Free energy dependence of rate constants for charge separation (k_{cs}, filled symbols) and charge recombination (k_{cr}, empty symbols) for contact charge transfer (●, ○) and bridge-mediated charge transfer (▲, Δ).

$$k_{et} = \frac{2\pi}{\hbar} \frac{H_{DA}^{\,2}}{\sqrt{4\pi\lambda_S k_B T}} e^{-S_c} \sum_{n=0}^{\infty} \frac{S_c^{\,n}}{n!} e^{-(\Delta G + \lambda_S + n\hbar\langle\omega_c\rangle)^2/4\lambda_S k_B T} \quad (5)$$

$$\text{where} \quad S_c = \frac{\lambda_i}{\hbar\langle\omega_c\rangle}$$

Boltzmann constant, T is the temperature (298 K), H_{DA} is the electronic coupling matrix element, S_c is the Huang–Rhys factor, ΔG is the free energy change (eq 3 or 4), λ_i is the nuclear reorganization energy, λ_s is the solvent reorganization energy, and $\langle\omega_c\rangle$ is the average high-frequency vibrational frequency.[19] A value of $\hbar\langle\omega_c\rangle = 1500$ cm^{-1} is assumed for electron-transfer processes involving aromatic molecules.[48,53] A fit to the entire data set is shown in Figure 6 and provides values of the solvent reorganization energy, λ_s, the nuclear reorganization energy, λ_i, and the electronic coupling matrix element, H_{DA}, reported in Table 1 (fit I).

The free energy dependence of intramolecular electron-transfer dynamics has been studied in numerous systems with fixed donor–acceptor geometry.[54] However, to our knowledge, only one system with a π-stacked donor–acceptor geometry, a cofacial cyclophane-bridged porphyrin–quinone system, has been previously investigated.[55,56] The electron-transfer parameters for this system are also reported in Table 1 (fit II). Both systems have relatively small values for λ_s in polar solvents, plausibly reflecting their compact structures which limit the contact of the donor and acceptor with the solvent. Both systems also have relatively large values of λ_i, reflecting changes in the molecular geometry which accompany the electron-transfer process. The value of H_{DA} for the hairpins is considerably larger than that for the porphyrin–quinone system. The driving force dependence of the dynamics of charge recombination has also been investigated for contact radical ion pairs formed upon excitation of Mulliken-type charge-transfer complexes. Gould and Farid[47,48] have estimated values of $H_{DA} = 750$ cm^{-1} and $\lambda_s = 0.48$ eV in acetonitrile solution, using a fixed value of $\lambda_i = 0.25$ eV. The increase in H_{DA} for the systems contact radical

Table 1. Electron Transfer Parameters from Fitting the Driving Force Dependence in Figure 6: (I) Fit for Nearest-Neighbor k_{cs} and k_{cr} Data, (II) Fit for a Cofacial Porphyrin−Quinone System, (III) Fit for a Contact Radical Ion Pair, and (IV) Fit for Bridge-Mediated k_{cs} and k_{cr} Data[a]

fit	λ_s, eV	λ_i, eV	H_{DA}, cm^{-1}
I[b]	0.23 ± 0.13	0.99 ± 0.12	347 ± 70
II[c]	0.26	0.53	133
III[d]	0.48	0.25	750
IV[b]	0.27 ± 0.09	1.03 ± 0.09	25 ± 4

[a] Parameters optimized with errors determined from fitting procedures using a value of $\hbar\langle\omega\rangle = 1500\ cm^{-1}$. [b] Data from ref 36. [c] Data from ref 55 for acetonitrile solution. [d] Data from ref 48 for acetonitrile solution obtained using a fixed value of $\lambda_i = 0.25$.

Chart 5. Decay Times of SE-Linked Hairpins

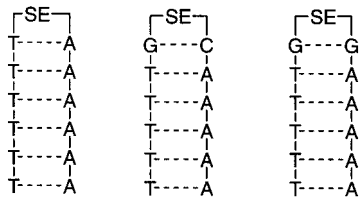

ion pairs > hairpins > porphyrin quinones parallels an increase in the donor−acceptor distance for these systems.

Donor−Acceptor Role Reversal

In most studies of photoinduced charge transfer involving nucleobases, a nucleobase is oxidized by an excited-state acceptor. Singlet pyrene[57] and coumarin[46] derivatives have been observed to oxidize guanine but reduce thymine or cytosine, which have the smallest reduction potentials of the common nucleobases (Chart 2). The SE diol has a low oxidation potential (Chart 1), and thus its singlet state would be expected to serve as a good electron donor but a poor acceptor.[42] Values of $\Delta G_{cs} = -0.17$ and -0.27 are calculated using eq 3 for quenching of singlet SE by C and T, respectively. The SE fluorescence is extensively quenched both in the hairpin T_6-SE-A_6 and in an analogue possessing a G:C base pair adjacent to the linker (Chart 5). In both cases, the formation and decay of the linker cation radical $SE^{+\bullet}$ is observed by transient absorption spectra. The singlet-state decay times (τ_s, Chart 5) provide values of $k_{cr} = 2.5 \times 10^{12}$ and $5.0 \times 10^{12}\ s^{-1}$ for quenching by an adjacent G:C and T:A base pair, respectively. The faster rate for the T:A base pair is consistent with its more negative value of ΔG_{cs}. Introduction of a GG mismatch adjacent to the SE linker results in a marked increase in the singlet decay time (Chart 5).[58] Evidently, singlet SE is not oxidized efficiently by guanine, in accord with a calculated value of $\Delta G_{cs} = +0.14$ eV.

Distance Dependence of Photoinduced Charge Transfer

As previously discussed, the strong SA fluorescence observed for the hairpin T_6-SA-A_6 is completely quenched upon introduction of a G:C base pair adjacent to the SA linker. For a family of hairpins containing a single G:C base pair at different positions relative to the linker (Chart 6), the SA fluorescence intensity increases as the distance between SA and G increases (Figure 7).[34,35] For the hairpin **5G:C**, which has four A:T base pairs between SA and G, there is ca. 10% quenching of the fluorescence intensity and the fluorescence decay time. Similar results are obtained for an *n*C:G family of hairpins in which the guanine donor is located in the polyA arm rather than the polyT arm.[59] Values of τ_s and τ_a have been determined for each of these hairpins by means of transient absorption spectroscopy (Chart 6).[35]

The rate constant for a bridge-mediated single-step superexchange electron-transfer process (Figure 1a) can

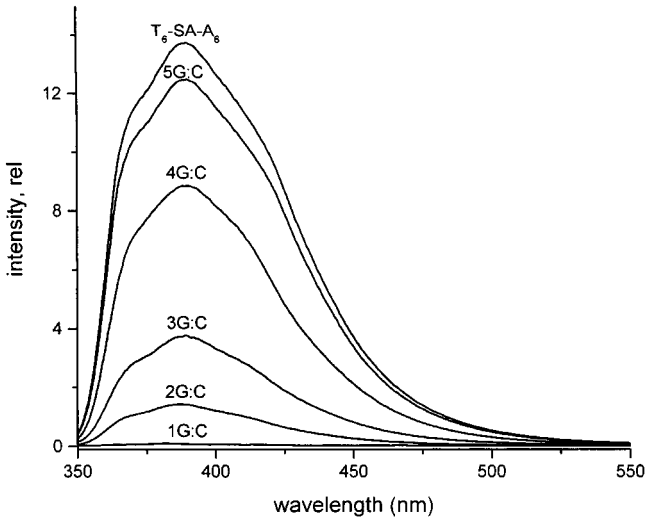

FIGURE 7. Fluorescence spectra of the T_6-SA-A_6 and the SA-linked nGC hairpins (Chart 6).

Chart 6. Decay Times of SA-Linked *n*G:C and *n*C:G Hairpins

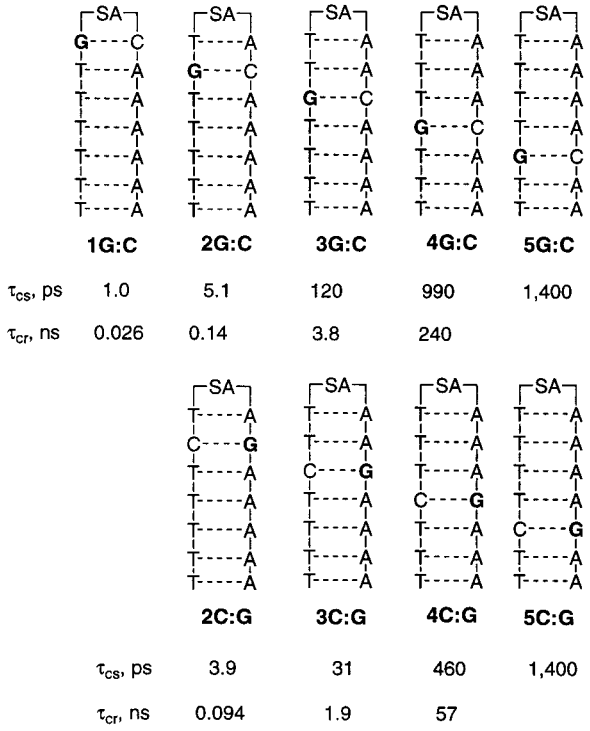

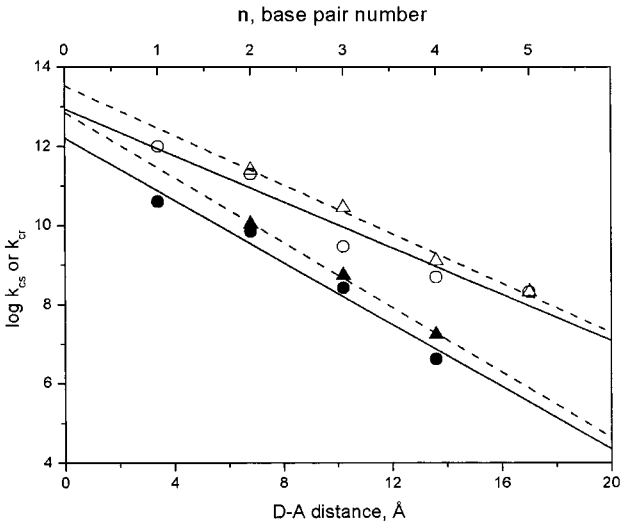

FIGURE 8. Distance dependence of the rate constants for charge separation (open symbols) and charge recombination (filled symbols) for SA-linked hairpin families (Chart 6) in which guanine is either in the polyT arm (e.g., 3G:C, ○, ●, solid lines) or in the polyA arm (e.g. 3C:G, Δ, ▲, dashed lines).

Table 2. Values of β and k_o for Charge Separation and Charge Recombination in Systems Where the Donor and Acceptor Are Separated by (T:A)$_n$ Base Pairs[a]

system	β, Å^{-1}	k_o, s^{-1}
*n*G:C hairpins, charge separation[a]	0.66	7.9×10^{12}
*n*C:G hairpins, charge separation[a]	0.71	1.6×10^{12}
*n*G:C hairpins, charge recombination[a]	0.90	3.2×10^{13}
*n*C:G hairpins, charge recombination[a]	0.94	6.3×10^{12}
covalent intercalated acridine[b]	1.5 (0.7)[c]	1.4×10^{10}
ethanoadenine[d]	1.0	
$G^{+\bullet}$ charge transport to GGG[e]	0.7	

[a] Data from ref 35. [b] Data from ref 61. [c] Data from ref 62. [d] Data from ref 63. [e] Data from ref 17.

be described by eq 5 if the bridge states lie well above the initial excited state.[19] The distance dependence of H_{DA} is related to the donor acceptor distance (R) by eq 6, where

$$H_{DA} = H_{DA}^{o} \exp(-\beta(R - R_o)/2) \qquad (6)$$

R_o is a reference geometry and β is a characteristic of the specific donor−bridge−acceptor system: the smaller the value of β, the more effective long-distance electron transfer. Simplification of eq 5 provides eq 1, the dependence of electron-transfer rate upon β, where the preexponential factor k_o is largely determined by the Franck−Condon factors for the electron-transfer process. Finally, β is dependent upon ΔE, the energy gap between the initial and bridge states, and the electronic mixing matrix element between adjacent bridge sites.

Plots of log(k_{cs}) and log(k_{cr}) vs the distance between the stilbene acceptor and guanine donor (calculated assuming a constant 3.4 Å π-stacking distance) are shown in Figure 8. The slopes and intercepts provide the values of β and k_o summarized in Table 2.[35] The values of β are similar for hairpins which have the guanine donor in the polyT or polyA arm (Chart 6). Values of β for charge separation are smaller than those for charge recombination in accord with a smaller energy gap, ΔE, between the initial and bridge states for the former process (0.2 vs 0.5 eV).

Chart 7. Structures of Hairpins with 3X:Y Quenchers

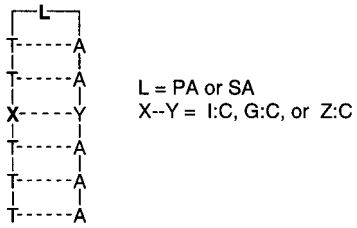

An alternative approach to the estimation of β is to determine the distance dependence of H_{DA} (eq 6).[36] To our knowledge, this approach has not previously been used in studies of the distance dependence of photoinduced electron transfer. The driving force dependence of k_{cs} and k_{cr} has been determined for five hairpins containing SA or PA linkers and a donor nucleobase separated from the linker by two T:A base pairs (Chart 7). The data are shown in Figure 6 along with the data for nearest-neighbor electron transfer. The electron-transfer parameters obtained from a fit of the data to eq 5 are reported in Table 1 (fit IV). The values of λ_s and λ_i are similar for nearest-neighbor and bridge-mediated electron transfer, suggesting that most of the change in geometry occurs in the hairpin loop region. The value of H_{DA} is significantly smaller for the bridge-mediated process, as expected for a superexchange electron-transfer process. A plot of the distance dependence of log(H_{DA}) vs R provides a value of $\beta = 0.77$ Å^{-1}, which is intermediate between the values in Table 2 obtained from the distance dependence of k_{cs} and k_{cr}.

Comparisons with Theory and Experiment

Our initial results for the distance dependence of charge-transfer dynamics[34] have been analyzed by Jortner et al.,[18] who conclude that they are consistent with a single-step superexchange mechanism. Beratan et al.[20,21] have investigated the distance dependence of electron transfer in several DNA model systems and report calculated values of β in the range 1.2−1.6 Å^{-1}. They have suggested that the smaller experimental values for our hairpin systems may reflect stronger coupling between the stilbene linker and (T:A)$_n$ bridge than assumed in their model calculations.[21] Calculations by Felts et al.[22] and by Davis et al.[23] indicate that an activated distance-independent mechanism may operate under specific conditions, particularly at distances longer than those that we have investigated.

Following our initial report of distance-dependent electron-transfer dynamics in DNA, several groups have reported related studies using variable numbers of T:A base pairs to separate an acceptor from a nucleobase donor. Tanaka and co-workers[60,61] have investigated DNA-mediated electron transfer in duplexes which possess a tethered acridine dye at a defined site. Quenching of the fluorescence intensity and lifetime by G:C base pairs at variable distances from the acridine provides values of β

$= 1.5$ Å^{-1} and $k_o = 1.9 \times 10^{12}$ s^{-1}. However, a reinvestigation of this system by Hess et al.[62] indicates that the strong distance dependence is a consequence of relaxation of the acridine chromophore, which is more rapid than electron transfer when there is one or more A:T base pair between the acridine acceptor and nucleobase donor. Thus, the actual value of β is likely to be much smaller than that reported by Tanaka and co-workers.[60,61] Kelly and Barton[63] have investigated quenching of the fluorescent base analogue 1-N^6-ethanoadenine (A_ϵ) by guanine or the more readily oxidized 7-deazaguanine (Chart 2). The distance dependence of the relative fluorescence intensity and the fluorescence decay times provides a value of $\beta = 1.0$ Å^{-1}. Poor coupling between the bulky A_ϵ acceptor and the adjacent base pair may be responsible for the relatively large value of β. Much weaker distance dependence is reported for quenching of the fluorescence of a 2-aminopurine acceptor; however, this observation has not been supported by direct spectroscopic observations of the products of electron transfer or by kinetic data.[63] Giese and co-workers[17] have used an ingenious method based on relative strand-cleavage efficiencies to study the distance dependence of single-step electron transfer from $G^{+\bullet}$ to a GGG sequence across an $(A:T)_n$ bridge and obtained a value of $\beta = 0.7$ Å^{-1}.

Harriman and co-workers[31,64] have investigated the dynamics of electron transfer from noncovalently attached intercalated donors to intercalated acceptors in duplex DNA. By assigning three of the multiple fluorescence decay components to donor−acceptor pairs separated by three, four, and five base pairs, they were able to obtain values of $\beta \approx 0.9-1.0$ Å^{-1} for charge separation and a larger value of $\beta \approx 1.5$ for charge recombination. Olson et al.[65] also have estimated a value of $\beta \approx 1$ Å^{-1} for electron transfer between noncovalent intercalated donors and acceptors.

In summary, values of β, the distance dependence of electron transfer in B-form DNA, appear to be converging in the range 0.6−1.0 Å^{-1}, smaller values reflecting smaller values of ΔE, the energy gap between the singlet acceptor and base pair bridge states. These β values are distinctly smaller than those reported for proteins and D−B−A systems with rigid hydrocarbon bridges ($\beta \approx 1.0-1.4$)[66,67] and are similar to those for D−B−A systems with linear conjugated bridges.[68] An example of wirelike behavior ($\beta < 0.1$) has recently been reported by Davis et al.[69] for D−B−A systems with *p*-phenylenevinylene oligomers as linkers in which the value of ΔE is minimized. While there have been claims of wirelike behavior in DNA,[5] they are not supported by direct kinetic measurements. The values of β summarized in Table 2 are consistent with relatively weak electronic interactions between the π-stacked bases in DNA, in accord with the calculations of Beratan and co-workers.[20,21]

Delocalization of Nucleobase Cation Radicals

Oxidative cleavage of DNA is known to occur preferentially at guanine, the most readily oxidized of the nucleobases.[9,10] Oxidative cleavage at guanine displays base-sequence selectivity, guanines adjacent to purine bases being more reactive than those with pyrimidine neighbors and GG or GGG sequences being more reactive than GA sequences.[70−72] The basis for this selectivity has been investigated computationally by Sugiyama and Saito.[73] Their results indicate that the ionization potential of guanine is lowered substantially by a neighboring purine, the effect being larger for guanine vs adenine and for a GGG vs a GG sequence (Table 3). Similar results were reported for G vs GG by Pratt et al.[74]

Table 3. Calculated Ionization Potentials, Relative Rate Constants for Charge Separation, and Charge Recombination, Relative Populations of Holes, Relative Yields of Strand Cleavage, and Relative Rates of Reaction Leading to Strand Cleavage for G, GG, and GGG Sequences

property of sequence	G	GG	GGG
IP, eV (calcd)[a]	7.51	7.28	7.07
k_{cs}, rel[b]	1.0	1.7	1.5
k_{cr}, rel[c]	1.0	0.33	0.23
$[G_n^{+\bullet}]$, rel[d]	1.0	7.7	20
k_{cl}, rel[e]	1.0	3.7	5.3
k_H^+, rel[f]	1.0	0.48	0.27

[a] Calculated ionization potentials for GA, GG, and GGG sequences from ref 73. [b] Relative rate constants for charge separation in hairpins **3C:G**, **3,4C:G**, and **3,4,5C:G** from Chart 9 ($k_{cs} = \tau_s^{-1}$). [c] Relative rate constants for charge recombination in hairpins **3C:G**, **3,4C:G**, and **3,4,5C:G** from Chart 9 ($k_{cr} = \tau_a^{-1}$). [d] Relative equilibrium populations of holes on G, GG, and GGG sequences from eq 8 and 9. [e] Relative yields of oxidative cleavage from ref 72. [f] Relative rates of guanine cation radical deprotonation at G, GG, and GGG sequences ($k_H^+ = k_{cl}/[G_n^{+\bullet}]$.

A lower oxidation potential for GA vs GT sequences might be expected to result in faster charge separation and charge recombination when guanine is located in the polyA vs polyT arm of an SA-linked hairpin. A smaller value of β might also be expected when guanine is located in the polyA vs polyT arm.[18] Larger values of k_{cr} and k_{cs} are observed for the *n*C:G vs *n*G:C hairpins (Chart 6) at short D−A separations, but no difference is observed at larger separations (Figure 8).[35] This results in values of β that are slightly larger for the C:G vs G:C hairpins (Table 2). Thus, the kinetic advantage for electron transfer via a polypurine vs polypyrimidine strand appears to be rather small and to operate only over short distances.

The dynamics of charge separation and charge recombination have also been investigated in several SA-linked hairpins possessing G, GG, and GGG sequences (Chart 8).[38] The resulting values of k_{cs} and k_{cr} for the hairpins **3,4C:G** and **3,5,6C:G** relative to the values for **3C:G** are reported in Table 3. Decreasing oxidation potential in the series G, GG, GGG should result in more negative values of ΔG_{cs} and hence an increase in k_{cs}. A small increase in k_{cs} is observed for GG vs G but not for GGG vs GG. A decrease in oxidation potential should also result in less negative values of ΔG_{cr} and hence an increase in k_{cr} for processes deep in the Marcus inverted region (Figure 5). However, a small decrease in k_{cr} is observed for the GGG or GG vs G. This may reflect delocalization of the hole over the GG or GGG sequence. However, the modest decreases in k_{cr}

Chart 8. Decay Times for SA-Linked Hairpins with G, GG, and GGG Sequences

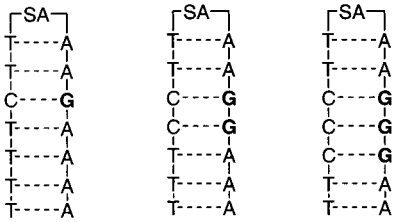

indicate that GG and GGG sequences do not function as deep hole traps. The small differences in the values of k_{cs} and k_{cr} for hairpins containing G, GG, and GGG sequences appear to be incompatible with the large differences in the calculated ionization potentials of these sequences (Table 3).

Dynamics and Equilibria for Hole Transport in DNA

Oxidative strand cleavage of guanine occurs selectively at guanine even under conditions where all of the nucleobases are oxidized.[9,10] Thus, cation radicals (holes) generated on other nucleobases must be able to migrate to guanine via a hole-transport process. In their studies of distance-dependent strand cleavage in DNA, Giese et al.[17] found that hole migration could occur over long distances when alternating A:T and G:C base pairs were used to separate the primary guanine hole donor and a GGG sequence. A plot of $\ln(\Phi_{rel})$ vs R, the distance between the primary guanine hole donor and the GGG sequence, has a slope $\beta' = 0.07$ Å^{-1}, significantly smaller than those for DNA-mediated superexchange electron transfer. This shallow distance dependence was attributed to a multistep hole-hopping mechanism (Figure 1b). By using a combination of hole hopping over several guanines and superexchange between neighboring guanines, both Bixon et al.[24] and Berlin et al.[25] have obtained excellent agreement between calculated and observed relative rate constants. Hole hopping involving multiple GG sequences has also been observed by Schuster et al.[16] and Núñez et al.[75]

Hairpins possessing SA linkers and multiple C:G base pairs (Chart 9) were designed to probe the dynamics of hole transport from $G^{+\bullet}$, formed via photoinduced charge transfer, to a GG or GGG sequence separated from $G^{+\bullet}$ by one T:A base pair.[37,38] According to the kinetic scheme shown in Figure 9, the singlet decay time of the SA linker (τ_s) should not be affected by the presence of a GG or GGG sequence remote from the linker. However, if hole transport competes with charge recombination of the initially formed $SA^{-\bullet}/G^{+\bullet}$ radical ion pair, then the $SA^{-\bullet}$ decay time (τ_a) should be affected. The values of τ_s for hairpins containing multiple C:G base pairs (Chart 9) are, in fact, similar to those of the hairpins containing a single C:G base pair (Chart 6). The value of τ_a for **2,4,5C:G** is similar

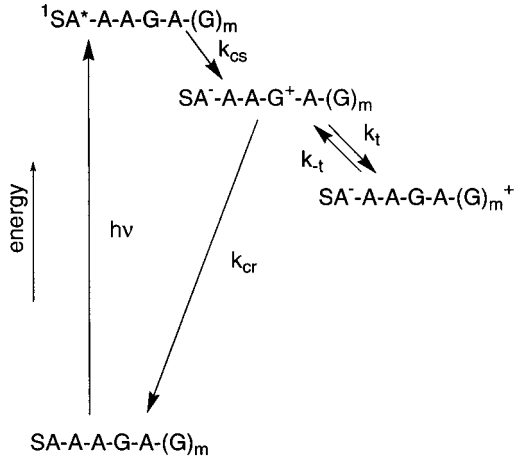

FIGURE 9. Kinetic scheme for charge separation (k_{cs}) and charge recombination (k_{cr}) in SA-linked hairpins which undergo hole transport (k_t and k_{-t}) to a more distal site containing multiple guanines. Only the guanine-containing arm of the hairpin is shown.

Chart 9. Decay Times for SA-Linked Hairpins with Hole Transport Sequences

to that for **2C:G**, indicative of the failure of hole transport to compete with charge recombination in $2G_3$ ($k_{cr} > k_t$). However, the values of τ_a for **4,6,7C:G** and **4,6,8,9C:G** are longer than that for **4C:G**, indicative of the occurrence of efficient hole transport ($k_t > k_{cr}$). Thus, the rate constant for hole transport is bracketed by the values of k_{cr} for **2C:G** and **4C:G** (1×10^{10} s$^{-1} > k_t > 2 \times 10^7$ s^{-1}).[37] The longer τ_a for **4,6,8,9C:G** vs **4,6,7C:G** suggests that multistep hole transport may compete with charge recombination.[58]

In the case of **3,5,6C:G** and **3,5,6,7C:G**, two decay components are observed for the anion radical, one shorter and one longer than that for **3C:G** (Chart 9), indicative of the occurrence of both charge recombination and hole transport. Nonlinear fitting of the $S^{-\bullet}$ decay data for **3,5,6C:G** using the exact analytical solution to this kinetic model in Figure 9 affords rate constants for forward and return hole transport of $k_t = (5.6 \pm 0.6) \times 10^7$ s^{-1} and $k_{-t} = (7.5 \pm 0.8) \times 10^6$ s^{-1}.[37] Similarly, analysis of the $S^{-\bullet}$ decay for **3,5,6,7C:G** affords values of $k_t = (8.7 \pm 1) \times 10^7$ s^{-1} and $k_{-t} = (4.3 \pm 0.1) \times 10^6$ s^{-1}.[38] These rate constants provide values for the equilibrium constants and free energies of reaction for the hole-transport processes, K_{ht} and ΔG_{ht} shown in eq 7 and 8.

$$G^{+\bullet} + GG \underset{k_{-t}}{\overset{k_t}{\rightleftharpoons}} G + GG^{+\bullet}$$

$$K_{ht} = 7.7 \pm 1, \Delta G_{ht} = -0.052 \pm 0.006 \quad (7)$$

$$G^{+\bullet} + GGG \underset{k_{-t}}{\overset{k_t}{\rightleftharpoons}} G + GGG^{+\bullet}$$

$$K_{ht} = 20 \pm 1, \Delta G_{ht} = -0.077 \pm 0.005 \quad (8)$$

Finally, a value of $\Delta G^\circ = -0.025 \pm 0.005$ eV for a hole localized on a GG vs GGG sequence is obtained by comparison of eqs 7 and 8.

These values of ΔG_{ht} are much smaller than the differences in calculated ionization potentials (Table 3) but are in good accord with a variety of experimental observations. First, they are consistent with the small differences in our values of k_{cs} and k_{cr} for hairpins which contain G, GG, and GGG sequences (Chart 8) and the small difference in the rate constants for oxidation of G vs GG sequences reported by Sistare et al.[76] Second, they are consistent with observations of hole transport between multiple GG sequences and between two GGG sequences.[16,71,75] Third, they are consistent with the modest selectivity observed for oxidative strand cleavage at GG or GGG vs G sequences. For example, Hickerson et al.[72] recently reported that oxidative cleavage of an 18-mer duplex containing G, GG, and GGG sequences occurred with a cleavage ratio of 1.0:3.7:5.3, respectively (Table 3). Using their cleavage data in combination with our equilibrium data provides relative rate constants for the chemical step (presumably proton transfer)[77] leading to strand cleavage at G, GG, and GGG sequences of 1:0.48:0.27. Thus, the chemical reactivity of a hole on guanine-containing sequences decreases as its stability increases.

The rather small effects of neighboring bases upon the dynamics and equilibria for charge-transfer (Chart 8) and charge-transport processes (Chart 9) suggests that hole delocalization occurs to only a limited degree in DNA. The relatively large π-stacking distance and limited orbital overlap in DNA are no doubt responsible for the weak interactions between both neutral and oxidized bases. These observations are consistent with a simple hole-hopping model for charge transport in DNA[24,25] and do not require the involvement of extensively delocalized polarons.[16]

Concluding Remarks

Synthetic hairpins with chromophore linkers have provided a versatile system for the investigation of photoinduced charge-transfer processes in B-form DNA. The synthetic strategy for hairpin synthesis has now been used to prepare several hundred hairpins with controlled base sequences and a variety of organic chromophores and one transition metal complex as linkers. Investigations of the dynamics of charge separation and charge recombination reactions involving the excited linker as acceptor and one or more donor nucleobases by means of transient absorption spectroscopy have provided heretofore unavailable details about the mechanisms of both single-step superexchange and multistep hole-transport processes. Our results are consistent with established theories of photoinduced electron transfer and hole transport and do not require the introduction of new paradigms.

In addition to providing an occasion for reviewing past accomplishments, preparation of this Account prompts us to consider the future. Can we elucidate the dynamics of electron injection and transport processes in DNA? Can either electron- or hole-transport processes occur efficiently over the long distances needed in a molecular electronic device? How fast are the chemical reactions which compete with hole or electron transport? We anticipate that the unique properties of synthetic hairpins will permits us to probe these and other challenging questions about the behavior of DNA.

We are deeply indebted to our students who have contributed to this project and to our colleagues Martin Egli and Mark Ratner for sharing their knowledge of DNA structure and electron-transfer phenomena, respectively. Financial support has been provided by grants from the Division of Chemical Sciences, Office of Basic Energy Sciences, U.S. Department of Energy (to F.D.L. and M.R.W.) and the National Institutes of Health (to R.L.L.).

References

(1) *Bioorganic Chemistry: Nucleic Acids*; Hecht, S. M., Ed.; Oxford University Press: Oxford, UK, 1996.
(2) Eley, D. D.; Spivey, D. I. T. Semiconductivity of Organic Substances. *Trans. Faraday Soc.* **1962**, *58*, 411−415.
(3) Murphy, C. J.; Arkin, M. R.; Ghatlia, N. D.; Bossmann, S.; Turro, N. J.; Barton, J. K. Fast photoinduced electron transfer through DNA intercalation. *Proc. Natl. Acad. Sci. U.S.A.* **1994**, *91*, 5315−5319.
(4) Arkin, M. R.; Stemp, E. D. A.; Holmlin, R. E.; Barton, J. K.; Hörmann, A.; Olson, E. J. C.; Barbara, P. F. Rates of DNA-mediated electron transfer between metallointercalators. *Science* **1996**, *273*, 475−479.
(5) Turro, N. J.; Barton, J. K. Paradigms, supermolecules, electron transfer and chemistry at a distance. What's the problem? The science or the paradigm? *J. Biol. Inorg. Chem.* **1998**, *3*, 201−209.
(6) Willner, I. Photoswitchable biomaterials: En route to optobioelectronic systems. *Acc. Chem. Res.* **1997**, *30*, 347−356.
(7) Fox, M. A. Fundamentals in the design of molecular electronic devices: Long-range charge carrier transport and electronic coupling. *Acc. Chem. Res.* **1999**, *32*, 201−207.
(8) Porath, D.; Bezryadin, A.; de Vries, S.; Dekker: C. Direct measurement of electrical transport through DNA molecules. *Nature* **2000**, *403*, 635−638.
(9) Armitage, B. Photocleavage of nucleic acids. *Chem. Rev.* **1998**, *98*, 1171−1200.
(10) Burrows, C. J.; Muller, J. G. Oxidative nucleobase modifications leading to strand scission. *Chem. Rev.* **1998**, *98*, 1109−1151.
(11) Holmlin, R. E.; Dandliker, P. J.; Barton, J. K. Charge transfer through the DNA base stack. *Angew. Chem., Int. Ed. Engl.* **1997**, *36*, 2714−2730.
(12) Kirsch-De Mesmaeker, A.; Lecomte, J.-P.; Kelly, J. M. Photoreactions of metal complexes with DNA, especially those involving a primary photo-electron transfer. *Top. Curr. Chem.* **1996**, *177*, 25−76.
(13) Tuite, E. In *Organic and Inorganic Photochemistry*; Ramamurthy, V., Schanze, K. S., Eds.; Marcel Dekker: New York, 1998; Vol. 2, pp 55−74.
(14) Barbara, P. F.; Olson, E. J. C. Experimental electron-transfer kinetics in DNA environment. *Adv. Chem. Phys.* **1999**, *107*, 647−676.
(15) Grinstaff, M. W. How do charges travel through DNA?—An update on a current debate. *Angew. Chem., Int. Ed.* **1999**, *38*, 3629−3635.
(16) Schuster, G. B. Long-range charge transfer in DNA: transient structural distortions control the distance dependence. *Acc. Chem. Res.* **2000**, *33*, 253−260.
(17) Giese, B. Long-distance charge transport in DNA: the hopping mechanism. *Acc. Chem. Res.* **2000**, *33*, 631−636.
(18) Jortner, J.; Bixon, M.; Langenbacher, T.; Michel-Beyerle, M. E. Charge transfer and transport in DNA. *Proc. Natl. Acad. Sci. U.S.A.* **1998**, *95*, 12759−12765.

(19) Bixon, M.; Jortner, M. Electron transfer−from isolated molecules to biomolecules. *Adv. Chem. Phys.* **1999**, *106*, 35−202.
(20) Priyadarshy, S.; Risser, S. M.; Beratan, D. N. DNA is not a molecular wire: protein-like electron-transfer predicted for an extended π-electron system. *J. Phys. Chem.* **1996**, *100*, 17678−17682.
(21) Priyadarshy, S.; Risser, S. M.; Beratan, D. N. DNA-mediated electron transfer. *J. Biol. Inorg. Chem.* **1998**, *3*, 196−200.
(22) Felts, A. K.; Pollard, W. T.; Friesner, R. A. Multilevel Redfield treatment of bridge-mediated lng-range electron transfer: a mechanism for anomalous distance dependence. *J. Phys. Chem.* **1995**, *99*, 2929−2940.
(23) Davis, W. B.; Wasielewski, M. R.; Ratner, M. A.; Mujica, V.; Nitzan, A. Electron-transfer rates in bridged molecular systems: a phenomenological approach to relaxation. *J. Phys. Chem.* **1997**, *101*, 6158−6164.
(24) Bixon, M.; Giese, B.; Wessely, S.; Langenbacher, T.; Michel-Beyerle, M. E.; Jortner, J. Long-range charge hopping in DNA. *Proc. Natl. Acad. Sci. U.S.A.* **1999**, *96*, 11713−11716.
(25) Berlin, Y. A.; Burin, A. L.; Ratner, M. A. On the long-range charge transfer in DNA. *J. Phys. Chem. A* **2000**, *104*, 443−445.
(26) Wilson, E. K. DNA: Insulator or wire? *Chem. Eng. News* **1997**, *75*, 33−38.
(27) Wilson, E. K. DNA's conductance still confounds. *Chem. Eng. News* **1998**, *75*, 51−54.
(28) Ratner, M. A. Electronic motion in DNA. *Nature* **1999**, *397*, 480−481.
(29) Salunkhe, M.; Wu, T.; Letsinger, R. L. Control of folding and binding of oligonucleotides by use of a nonnucleotide linker. *J. Am. Chem. Soc.* **1992**, *114*, 8768−8772.
(30) Letsinger, R. L.; Wu, T. Use of a stilbenedicarbxoamide bridge in stabilizing, monitoring, and photochemically altering folded conformations of oligonucleotides. *J. Am. Chem. Soc.* **1995**, *117*, 7323−7328.
(31) Brun, A. M.; Harriman, A. Dynamics of electron transfer between intercalated polycyclic molecules: effect of interspersed bases. *J. Am. Chem. Soc.* **1992**, *114*, 3656−3660.
(32) Meade, T. J.; Kayyem, J. F. Electron transfer through DNA: Site-specific modification of duplex DNA with ruthenium donors and acceptors. *Angew. Chem., Int. Ed. Engl.* **1995**, *34*, 352−354.
(33) Murphy, C. J.; Arkin, M. R.; Jenkins, Y.; Ghatlia, N. D.; Bossmann, S. H.; Turro, N. J.; Barton, J. K. Long-range photoinduced electron transfer through a DNA helix. *Science* **1993**, *262*, 1025−1029.
(34) Lewis, F. D.; Wu, T.; Zhang, Y.; Letsinger, R. L.; Greenfield, S. R.; Wasielewski, M. R. Distance-dependent electron transfer in DNA hairpins. *Science* **1997**, *277*, 673−676.
(35) Lewis, F. D.; Wu, T.; Liu, X.; Letsinger, R. L.; Greenfield, S. R.; Miller, S. E.; Wasielewski, M. R. Dynamics of photoinduced charge separation and charge recombination in synthetic DNA hairpins with stilbenedicarboxamide linkers. *J. Am. Chem. Soc.* **2000**, *122*, 2889−2902.
(36) Lewis, F. D.; Kalgutkar, R. S.; Wu, Y.; Liu, X.; Liu, J.; Hayes, R. T.; Miller, S. E.; Wasielewski, M. R. Driving force dependence of electron transfer dynamics in synthetic DNA hairpins. *J. Am. Chem. Soc.* **2000**, *122*, 12346−12351.
(37) Lewis, F. D.; Liu, X.; Liu, J.; Miller, S. E.; Hayes, R. T.; Wasielewski, M. R. Direct measurement of hole transport dynamics in DNA. *Nature* **2000**, *406*, 51−53.
(38) Lewis, F. D.; Liu, X.; Liu, J.; Hayes, R. T.; Wasielewski, M. R. Dynamics and equilibria for oxidation of G, GG, and GGG sequences in DNA Hairpins. *J. Am. Chem. Soc.* **2000**, *122*, 12037−12038.
(39) Lewis, F. D.; Zhang, Y.; Liu, X.; Xu, N.; Letsinger, R. L. Naphthalenedicarboxamides as fluorescent probes of inter- and intramolecular electron transfer in single strand, hairpin, and duplex DNA. *J. Phys. Chem. B* **1999**, *103*, 2570−2578.
(40) Lewis, F. D.; Liu, X.; Miller, S. E.; Wasielewski, M. R. Electronic interactions between π-stacked DNA base pairs and diphenylacetylene-4,4′-dicarboxamide in hairpin DNA. *J. Am. Chem. Soc.* **1999**, *121*, 9746−9747.
(41) Bevers, S.; Schutte, S.; McLaughlin, L. W. Naphthalene- and perylene-based linkers for the stabilization of hairpin triplexes. *J. Am. Chem. Soc.* **2000**, *122*, 5905−5915.
(42) Lewis, F. D.; Liu, X.; Wu, Y.; Miller, S. E.; Wasielewski, M. R.; Letsinger, R. L.; Sanishvili, R.; Joachimiak, A.; Tereshko, V.; Egli, M. Structure and photoinduced electron transfer in exceptionally stable synthetic DNA hairpins with stilbenediether linkers. *J. Am. Chem. Soc.* **1999**, *121*, 9905−9906.
(43) Lewis, F. D.; Liu, X. Phototriggered DNA hairpin formation in a stilbenediether-linked bis(oligonucleotide) conjugate. *J. Am. Chem. Soc.* **1999**, *121*, 11928−11929.
(44) Lewis, F. D.; Helvoigt, S. A.; Letsinger, R. L. Synthesis and spectroscopy of Ru(II)-bridged DNA hairpins. *Chem. Commun.* **1999**, 327−328.
(45) Linker singlet energies are determined from the intersection of absorption and fluorescence spectra. Linker oxidation potentials are measured vs SCE in dimethyl sulfoxide solution.
(46) Seidel, C. A. M.; Schulz, A.; Sauer, M. H. M. Nuclobase-specific quenching of fluorescent dyes. 1. Nucleobase one-electron redox potentials and their correlation with static and dynamic quenching efficiencies. *J. Phys. Chem.* **1996**, *100*, 5541−5553.
(47) Gould, I. R.; Young, R. H.; Moody, R. E.; Farid, S. Contact and solvent-separated geminate radical ion pairs in electron-transfer photochemistry. *J. Phys. Chem.* **1991**, *95*, 2068−2080.
(48) Gould, I. R.; Farid, S. Dynamics of bimolecular photoindicued electron-transfer reactions. *Acc. Chem. Res.* **1996**, *29*, 522−528.
(49) Hubig, S. M.; Bockman, T. M.; Kochi, J. K. Optimized electron transfer in charge-transfer ion pairs. Pronounced inner-sphere behavior of olefin donors. *J. Am. Chem. Soc.* **1996**, *118*, 3842−3851.
(50) Weller, A. Photoinduced electron transfer in solution: exciplex and radical ion pair formation free enthalpies and their solvent dependence. *Z. Phys. Chem. Neue. Folg.* **1982**, *133*, 93−98.
(51) Candeias, L. P.; Steenken, S. Structure and acid−base properties of one-electron-oxidized deoxyguanosine, guanosine, and 1-methylguanosine. *J. Am. Chem. Soc.* **1989**, *111*, 1094−1099.
(52) Marcus, R. A. On the theory of oxidation−reduction reactions involving electron transfer. I. *J. Chem. Phys.* **1956**, *24*, 966−978.
(53) Closs, G. L.; Miller, J. R. Intramolecular long-distance electron transfer in organic molecules. *Science* **1988**, *240*, 440−447.
(54) Wasielewski, M. R. Photoinduced electron transfer in supramolecular systems for artificial photosynthesis. *Chem. Rev.* **1992**, *92*, 435−461.
(55) Häberle, T.; Hirsch, J.; Pöllinger, F.; Heitele, H.; Michel-Beyerle, M. E.; Anders, C.; Döhling, A.; Krieger, C.; Rückermann, A.; Staab, H. A. Ultrafast charge separation and driving force dependence in cyclophane-bridged Zn-porphyrin-quinone molecules. *J. Phys. Chem.* **1996**, *100*, 18269−18274.
(56) Pöllinger, F.; Musewald, C.; Heitele, H.; Michele-Beyerle, M. E. Photoinduced electron transfer in cyclophane-bridged porphyrin-quinone molecules. A subpicosecond transient absorption study. *Ber. Bunsen-Ges. Phys. Chem.* **1996**, *100*, 2076−2080.
(57) Shafirovich, V. Y.; Courtney, S. H.; Ya, N.; Geacintov, N. E. Proton-coupled photoinduced electron transfer, deuterium isotope effects, and fluorescence quenching in noncovalent benzo[*a*]-pyrenetetraol-nucleoside complexes in aqueous solutions. *J. Am. Chem. Soc.* **1995**, *117*, 4920−4929.
(58) Lewis, F. D.; Wasielewski, M. R. Unpublished results.
(59) Lewis, F. D.; Letsinger, R. L. Distance-dependent photoinduced electron transfer in synthetic single-strand and hairpin DNA. *J. Biol. Inorg. Chem.* **1998**, *3*, 215−221.
(60) Fukui, K.; Tanaka, T. Distance dependence of photoinduced electron transfer in DNA. *Angew. Chem., Int. Ed.* **1998**, *37*, 158−161.
(61) Fukui, K.; Tanaka, K.; Fujitsuka, M.; Watanabe, A.; Ito, O. Distance dependence of electron transfer in acridine-intercalated DNA. *J. Photochem. Photobiol. B: Biol.* **1999**, *50*, 18−27.
(62) Hess, S.; Götz, M.; Davis, W. B.; Michel-Beyerle, M. E. Unpublished results.
(63) Kelley, S. O.; Barton, J. K. Electron transfer between bases in double helical DNA. *Science* **1999**, *283*, 375−381.
(64) Harriman, A. Electron tunneling in DNA. *Angew. Chem., Int. Ed.* **1999**, *38*, 945−949.
(65) Olson, E. J. C.; Hu, D.; Hörmann, A.; Barbara, P. F. Quantitative modeling of DNA-mediated electron transfer between metallo-intercalators. *J. Phys. Chem.* **1997**, *101*, 299−303.
(66) Winkler, J. R.; Gray, H. B. Electron transfer in ruthenium-modified proteins. *Chem. Rev.* **1992**, *92*, 369−379.
(67) Johnson, M. D.; Miller, J. R.; Green, N. S.; Closs, G. L. Distance dependence of intramolecular hole and electron transfer in organic radical ions. *J. Phys. Chem.* **1989**, *93*, 1173−1176.
(68) Tolbert, L. M. Solitons in a box: the organic chemistry of electrically conducting polyenes. *Acc. Chem. Res.* **1992**, *25*, 561−568.
(69) Davis, W. B.; Svec, W. A.; Ratner, M. A.; Wasielewski, M. R. Molecular-wire behaviour in *p*-phenylenevinylene oligomers. *Nature* **1998**, *396*, 60−63.
(70) Saito, I.; Takayama, M.; Sugiyama, H.; Nakatani, K. Photoinduced DNA cleavage via electron transfer: demonstration that guanine residues located 5′ to guanine are the most electron-donating sites. *J. Am. Chem. Soc.* **1995**, *117*, 6406−6407.
(71) Nakatani, K.; Dohno, C.; Saito, I. Modulation of DNA-Mediated Hole-Transport Efficiency by Changing Superexchange Electronic Interaction. *J. Am. Chem. Soc.* **2000**, *122*, 5893−5894.
(72) Hickerson, R. P.; Prat, F.; Muller, J. G.; Foote, C. S.; Burrows, C. J. Sequence and stacking dependence of 8-oxoguanine oxidation: comparison of one-electron vs singlet oxygen mechanisms. *J. Am. Chem. Soc.* **1999**, *121*, 9423−9428.

(73) Sugiyama, H.; Saito, I. Theoretical studies of GG-specific photocleavage of DNA via electron transfer: significant lowering of ionization potential and 5′-localization of HOMO of stacked GG bases in B-form DNA. *J. Am. Chem. Soc.* **1996**, *118*, 7063−7068.
(74) Prat, F.; Houk, K. N.; Foote, C. S. Effect of guanine stacking on the oxidation of 8-oxoguanine in B-DNA. *J. Am. Chem. Soc.* **1998**, *120*, 845−846.
(75) Núñez, M. E.; Hall, D. B.; Barton, J. K. Long-range oxidative damage to DNA: effects of distance and sequence. *Chem., Biol.* **1999**, *6*, 85−97.
(76) Sistare, M. F.; Codden, S. J.; Heimlich, G.; Thorp, H. H. Effects of base stacking on guanine electron transfer: Rate constants for G and GG sequences of oligonucleotides from catalytic electrochemistry. *J. Am. Chem. Soc.* **2000**, *122*, 4742−4749.
(77) Steenken, S. Electron transfer in DNA? Competition by ultra-fast proton transfer? *Biol. Chem.* **1977**, *378*, 1293−1297.

AR0000197